ON THE PROBLEM OF THE DIAGNOSTIC CALCULATION OF VERTICAL AND RADIAL MOTIONS IN A WET VORTEX

STANLEY L. ROSENTHAL

National Hurricane Center, U.S. Weather Bureau, Miami, Fla.

[Manuscript received April 15, 1963; revised July 5, 1963]

ABSTRACT

In the treatment of numerical models of symmetrical vortices, balanced radial and vertical velocity components may be obtained from a diagnostic equation first derived by Eliassen. However, when this equation is applied to vortices which resemble tropical cyclones, one finds hyperbolicity in regions where saturated ascent is accompanied by conditional static instability. Eliassen suggests that the equation can, nevertheless, be solved as a boundary-value problem through an iterative technique and predicts that the iterations will produce a solution in the form of a convergent geometric series. We have applied Eliassen's procedure to two vortices. For the first of these, we obtained the numerical values of the first three terms in the series. The results do not confirm Eliassen's suggestion concerning the behavior of the ratio of successive terms in the series. In the second case, 27 terms of the series were obtained. Here, convergence does appear to take place but not in the manner predicted by Eliassen's geometric formula.

1. INTRODUCTION

Staff members of the National Hurricane Research Project are currently conducting numerical experiments with a model designed to study the intensification of warm-core tropical cyclones. To obtain balanced initial conditions, the initial vertical and radial wind components, in the form of a Stokes stream function, are obtained by a diagnostic procedure developed by Eliassen [1, 2, 3] and recently applied to tropical cyclones by Estoque [4]. Eliassen's procedure leads to a second order, linear, partial differential equation for the stream function. In the cases which we have treated, the diagnostic equation is hyperbolic in regions where saturated ascent is accompanied by conditional static instability.

According to Eliassen [3], it may be possible to circumvent this difficulty as follows. A solution for a dry atmosphere should first be obtained. The latent heat term should then be calculated from the dry vertical motions and used as a forcing function to obtain a second solution to the diagnostic equation. The latent heat term is recalculated on the basis of the vertical motions obtained from the second solution. A third solution to the diagnostic equation is then obtained and so on. Eliassen [3] argued that the successive corrections would form a convergent geometric series provided that the lapse rate did not approach the dry adiabatic lapse rate. If this is indeed so, the solution to the problem could be obtained from the dry solution and the first two wet corrections. The calculations reported on below shed some light on the validity of Eliassen's method.

2. THE DIAGNOSTIC MODEL

We treat a circularly symmetrical model. At the initial instant, and for a short period thereafter, we assume gradient balance. But use of cylindrical coordinates,

$$\frac{v_\theta^2}{r}+fv_\theta=\theta\frac{\partial\phi}{\partial r}. \tag{1}$$

v_θ is the tangential wind component, r is the radial coordinate, f is the Coriolis parameter. θ is the potential temperature and ϕ is defined by

$$\phi=c_p\left(\frac{p}{p_0}\right)^{\frac{R}{c_p}} \tag{2}$$

where p is pressure, p_0 is 1000 mb., R is the specific gas constant for dry air, and c_p is the specific heat capacity at constant pressure for dry air. The absolute angular momentum per unit mass,

$$M_a=rv_\theta+f\frac{r^2}{2} \tag{3}$$

is used to eliminate v_θ from equation (1). This gives

$$\frac{\partial\phi}{\partial r}=r^{-3}\theta^{-1}\left(M_a^2-f^2\frac{r^4}{4}\right). \tag{4}$$

Equation (4) is differentiated with respect to time (t) and then with respect to height (z) to give

$$r^3\theta\frac{\partial\phi}{\partial r}\frac{\partial^2\theta}{\partial z\partial t}+r^3g\frac{\partial^2\theta}{\partial r\partial t}-\frac{\partial M_a^2}{\partial z}\frac{\partial\theta}{\partial t}-\theta\frac{\partial^2 M_a^2}{\partial z\partial t}+\frac{\partial\theta}{\partial z}\frac{\partial M_a^2}{\partial t}=0. \tag{5}$$

The hydrostatic equation, in the form

$$\frac{\partial\phi}{\partial z}=-\frac{g}{\theta}, \tag{6}$$

where g is the acceleration due to apparent gravity, was used to eliminate $(\partial^2\phi)/(\partial r\partial z)$. The first law of thermodynamics

$$\frac{\partial\theta}{\partial t}=-v_r\frac{\partial\theta}{\partial r}-w\frac{\partial\theta}{\partial z}-\frac{w\gamma L}{\phi}=\frac{\partial q_{ss}}{\partial z}+\frac{c_p}{\rho_s\phi}\frac{\partial}{\partial z}\left(\rho_s K_z\frac{\partial\theta}{\partial z}\right)+\frac{c_p}{\phi}r^{-1}K_H\frac{\partial}{\partial r}\left(r\frac{\partial\theta}{\partial r}\right), \tag{7}$$

and the tangential equation of motion, in the form

$$\frac{\partial M_a^2}{\partial t}=-v_r\frac{\partial M_a^2}{\partial r}-w\frac{\partial M_a^2}{\partial z}+2M_a\left[\frac{1}{\rho_s}\frac{\partial}{\partial z}\left(\rho_s K_z\frac{\partial M_a^2}{\partial z}\right)+rK_H\frac{\partial\zeta}{\partial r}\right], \tag{8}$$

are now introduced. In equations (7) and (8), v_r is the radial wind component, w is the vertical wind component, γ is a parameter to be discussed in section 4, q_{ss} is the saturation specific humidity for the mean tropical atmosphere, ρ_s is the dry density of the mean tropical atmosphere, L is the latent heat of vaporization, K_z is the Austausch coefficient for the vertical mixing of both heat and momentum (assumed to be at most a function of height), K_H is the Austausch coefficient for lateral mixing of heat and momentum (assumed constant), ζ is the relative vorticity,

$$\zeta=\frac{\partial v_\theta}{\partial r}+\frac{v_\theta}{r}. \tag{9}$$

The equation of continuity is taken in the form

$$\frac{\partial(\rho_s wr)}{\partial z}+\frac{\partial(\rho_s v_r r)}{\partial r}=0. \tag{10}$$

From (10), we obtain

$$w=\frac{1}{\rho_s r}\frac{\partial\psi}{\partial r} \tag{11}$$

and

$$v_r=-\frac{1}{\rho_s r}\frac{\partial\psi}{\partial z} \tag{12}$$

where ψ is the Stokes stream function.

Equations (7) and (8) are used to eliminate $\frac{\partial^2\theta}{\partial z\partial t}$, $\frac{\partial^2\theta}{\partial r\partial t}$, $\frac{\partial\theta}{\partial t}$, $\frac{\partial^2 M_a^2}{\partial z\partial t}$ and $\frac{\partial M_a^2}{\partial t}$ from equation (5). Next, equations (11) and (12) are used to eliminate v_r and w from the resulting equation. The latent heat term is, however, left unmodified. These manipulations yield

$$A\frac{\partial^2\psi}{\partial z^2}+B\frac{\partial^2\psi}{\partial z\partial r}+C\frac{\partial^2\psi}{\partial r^2}+D\frac{\partial\psi}{\partial z}+E\frac{\partial\psi}{\partial r}+F+G+L^*=0, \tag{13}$$

where

$$A=\theta\left[r^3\frac{\partial\phi}{\partial r}\frac{\partial\theta}{\partial r}-\frac{\partial M_a^2}{\partial r}\right], \tag{14}$$

$$B=2r^3g\frac{\partial\theta}{\partial r}, \tag{15}$$

$$C=-r^3g\frac{\partial\theta}{\partial z}, \tag{16}$$

$$D=-r^2\left[4g+\frac{r\theta}{\rho_s}\frac{\partial\rho_s}{\partial z}\frac{\partial\phi}{\partial r}\right]\frac{\partial\theta}{\partial r}+f^2r^3\frac{\partial\theta}{\partial z}+\frac{\theta}{\rho_s}\frac{\partial\rho_s}{\partial z}\frac{\partial M_a^2}{\partial r}, \tag{17}$$

$$E=r^2g\left[\frac{\partial\theta}{\partial z}-\frac{r}{\rho_s}\frac{\partial\rho_s}{\partial z}\frac{\partial\theta}{\partial r}\right], \tag{18}$$

$$F=\rho_s r\left[H\frac{\partial\theta}{\partial z}-\theta\frac{\partial H}{\partial z}\right], \tag{19}$$

$$G=\rho_s r^4\left[g\frac{\partial J}{\partial r}+\theta\frac{\partial\phi}{\partial r}\frac{\partial J}{\partial z}-\frac{1}{r^3}\frac{\partial M_a^2}{\partial z}J\right], \tag{20}$$

and

$$L^*=\rho_s r^4\left[\frac{1}{r^3}\frac{\partial M_a^2}{\partial z}\left(\frac{w\gamma L}{\phi}\frac{\partial q_{ss}}{\partial z}\right)-\theta\frac{\partial\phi}{\partial r}\frac{\partial}{\partial z}\left(\frac{w\gamma L}{\phi}\frac{\partial q_{ss}}{\partial z}\right)-g\frac{\partial}{\partial r}\left(\frac{w\gamma L}{\phi}\frac{\partial q_{ss}}{\partial z}\right)\right]. \tag{21}$$

In equation (19),

$$H=2M_a\left[\frac{1}{\rho_s}\frac{\partial}{\partial z}\left(\rho_s K_z\frac{\partial M_a}{\partial z}\right)+rK_H\frac{\partial\zeta}{\partial r}\right]; \tag{22}$$

in equation (20),

$$J=\frac{c_p}{\rho_s\phi}\frac{\partial}{\partial z}\left(\rho_s K_z\frac{\partial\theta}{\partial z}\right)+\frac{c_pK_H}{\phi r}\frac{\partial}{\partial r}\left(r\frac{\partial\theta}{\partial r}\right). \tag{23}$$

For dry motion, equation (13) is elliptic if $B^2-4AC<0$. (Cases in which $B^2-4AC>0$ will not be considered here.) In the case of saturated ascent, Eliassen suggests that we proceed as follows. A solution of (13), ψ_0, is obtained by setting L^* equal to zero. A first estimate of L^* is then calculated from ψ_0. A second solution, $\psi_1=\psi_0+\Delta_1\psi$, is obtained. A second estimate of L^* is evaluated from ψ_1 and a third solution, $\psi_2=\psi_1+\Delta_2\psi$, is obtained and so on. The desired solution of equation (13) is then assumed to be given by

$$\psi=\psi_0+\Delta_1\psi+\Delta_2\psi+\ \ldots\ +\Delta_\nu\psi+\ \ldots \tag{24}$$

According to Eliassen [3], this series is geometric and will converge if the lapse rate is not close to the dry adiabatic lapse rate. Hence,

$$\psi=\psi_0+\frac{\Delta_1\psi}{1-k},\qquad 0<k<1. \tag{25}$$

Furthermore, Eliassen's analysis [3] indicates that k should be about 0.5 in regions where updrafts take place with

neutral buoyancy. Also, Eliassen predicts that k should vary inversely with the static stability.

3. BOUNDARY CONDITIONS

A difference analogue to (13) has been applied to the region of the r–z plane delineated by

$$0 \leq r \leq R_0, \qquad 0 \leq z \leq H$$

R_0 is 1000 km. and H is the 100-mb. height of the mean tropical atmosphere (also assumed to be the height of the tropopause). The meridional circulation is assumed to be closed with the boundary taken as the $\psi=0$ streamline.

To evaluate the forcing functions, F and G, certain additional boundary conditions were assumed. At $z=0$, we took

$$\rho_s K_z \frac{\partial v_\theta}{\partial z} = \rho_s C_D |v_\theta| v_\theta, \tag{26}$$

$$\rho_s K_z \frac{\partial \theta}{\partial z} = \rho_s C_D (T - T_{sea}) |v_\theta| \tag{27}$$

where C_D is the drag coefficient, T_{sea} is the sea-surface temperature, and T is the air temperature. In equations (26) and (27), we have assumed that the error made by replacing the total wind speed with $|v_\theta|$ is small compared to the error due to the uncertainty in the evaluation of C_D. At $z=H$, we assume

$$\rho_s K_z \frac{\partial v_\theta}{\partial z} = 0, \tag{28}$$

$$T - T_s = 0, \tag{29}$$

and

$$\frac{\partial}{\partial z}(T - T_s) = 0, \tag{30}$$

where T_s is the temperature of the mean tropical atmosphere. Equations (29) and (30) imply

$$\left(\rho_s K_z \frac{\partial \theta}{\partial z}\right)_{z=H} = \left[\frac{\rho_s K_z \theta_s}{T_s}\left(\frac{\partial T_s}{\partial z} - \frac{g}{c_p}\right)\right]_{z=H}. \tag{31}$$

Equations (26) and (28) were used in the evaluation of F while (27) and (31) were used in obtaining G. In the experiments reported on below, K_H was set equal to zero. Hence, there was no need to apply special conditions to the lateral mixing terms.

4. COMPUTATION OF LATENT HEATING

For reasons of simplicity, all ascending air is assumed to be saturated with water vapor. All changes of phase, regardless of temperature, are assumed to be from vapor to liquid. In the calculations discussed below, the term

$$S = -w\left(\frac{\partial \theta}{\partial z} + \frac{\gamma L}{\phi}\frac{\partial q_{ss}}{\partial z}\right) \tag{32}$$

of equation (7) is treated as follows. When w is positive,

$$S' = \frac{\partial \theta}{\partial z} + \frac{L}{\phi}\frac{\partial q_{ss}}{\partial z}$$

is tested for sign. If S' is positive, S is calculated with $\gamma=1$. However, if S' is negative, S is set equal to zero. Physically, this amounts to the assumption that not all of the released latent heat warms the dry air but rather that a certain portion of it is used to evaporate liquid water. If L^* (in equation (13)) were evaluated explicitly in terms of ψ, the coefficient, C, would be zero at the points where S was set to zero. Hence, our procedure produces weaker hyperbolicity than would otherwise be the case. However, as noted earlier, Eliassen suggested that $k=0.5$ only for the case where $C=0$.

The preceding discussion establishes the following values for the parameter γ.

$\gamma=0$ if $w \leq 0$

$\gamma=1$ if $w>0$ and $S' \geq 0$

$\gamma = -\frac{\phi}{L}\left(\frac{\partial \theta}{\partial z}\Big/\frac{\partial q_{ss}}{\partial z}\right)$ if $w>0$ and $S' \leq 0$.

5. NUMERICAL TECHNIQUES

A rectangular grid in the r–z plane was employed. This grid consisted of 31 points (rows) in the vertical direction which were spaced at 550 m. and 26 points (columns) in the radial direction. Radial spacing was 40 km. The subscript i is introduced to denote row and the subscript j will denote column. With this, our finite difference analogue to equation (13) may be written

$$\begin{aligned}
&\frac{A_{i,j}}{\Delta z^2}(\psi_{i+1,j}+\psi_{i-1,j}-2\psi_{i,j}) + \frac{B_{i,j}}{4\Delta z \Delta r}(\psi_{i+1,j+1}-\psi_{i+1,j-1} \\
&\quad -\psi_{i-1,j+1}+\psi_{i-1,j-1}) + \frac{C_{i,j}}{\Delta r^2}(\psi_{i,j+1}+\psi_{i,j-1}-2\psi_{i,j}) \\
&\quad + \frac{D_{i,j}}{2\Delta z}(\psi_{i+1,j}-\psi_{i-1,j}) + \frac{E_{i,j}}{2\Delta r}(\psi_{i,j+1}-\psi_{i,j-1}) \\
&\quad + F_{i,j} + G_{i,j} + L^*_{i,j} = 0. \\
&\qquad i=1,\ 2,\ \ldots,\ 29,\ j=1,\ 2,\ \ldots,\ 24.
\end{aligned} \tag{33}$$

This system of equations was solved by relaxation. The correction formula employed was

$$\psi_{i,j}^{(n+1)} = \psi_{i,j}^{(n)} + \frac{(\text{RESIDUAL})_{i,j}^{(n)}}{2\left(\frac{A_{i,j}}{\Delta z^2}+\frac{C_{i,j}}{\Delta r^2}\right)} \tag{34}$$

where the superscript, (n), denotes the scan count. A relaxation was terminated when the $\psi_{i,j}^{(n+1)}$ were such that no $v_r^{(n+1)}$ differed from $v_r^{(n)}$ by more than 10^{-2} m. sec.$^{-1}$ and no $w^{(n+1)}$ differed from $w^{(n)}$ by more than 10^{-3} m. sec.$^{-1}$.

6. EXPERIMENT I

Table 1 gives standard temperatures for each row of our grid. These were modeled from Jordan's [5] mean tropical atmosphere. Figure 1 shows departures from these standard temperatures for a hypothetical vortex. The pressure field for this vortex was obtained by an integration of the hydrostatic equation with the assumption that the top row of the grid was the 100-mb. surface. Figure 2 shows the sea level pressure profile. The gradient wind distribution is illustrated by figure 3. For this experiment, C_D was set equal to 2.4×10^{-3} and K_z was taken as a linear function of height with a value of 50 m.^{2} sec.$^{-1}$ at $z=0$ and a value of zero at 100 mb. The sea-surface temperature (T_{sea}) was set equal to the sea level air temperature.

Figure 4 shows[1] (a) ψ_0, (b) $\psi_1=\psi_0+\Delta_1\psi$, and (c) $\psi_2=\psi_0+\Delta_1\psi+\Delta_2\psi$. The reader should note the increased strength of the meridional circulation and the upward progression of the main upper return current as successive corrections

[1] During the calculations for Experiment I, a magnetic tape failure occurred just after the completion of the ψ_2 evaluation. Because of a change in the design of our prognostic experiment, we lost interest in this vortex and, as a result, the diagnostic calculation was not restarted and, hence, not carried to its logical conclusion.

TABLE 1.—*Temperatures of the mean tropical atmosphere as a function of height*

Height (meters)	Row	Temperature (° C.)	Height (meters)	Row	Temperature (° C.)
0	0	299.4	8,800	16	245.5
550	1	295.5	9,350	17	241.0
1,100	2	292.5	9,900	18	236.8
1,650	3	289.0	10,450	19	232.3
2,200	4	286.0	11,000	20	228.0
2,750	5	283.0	11,550	21	223.8
3,300	6	279.8	12,100	22	219.5
3,850	7	276.5	12,650	23	215.5
4,400	8	273.7	13,200	24	211.2
4,950	9	270.7	13,750	25	207.8
5,500	10	267.5	14,300	26	205.0
6,050	11	264.0	14,850	27	202.5
6,600	12	260.7	15,400	28	201.3
7,150	13	257.3	15,950	29	200.7
7,700	14	253.7	16,500	30	200.2
8,250	15	249.7			

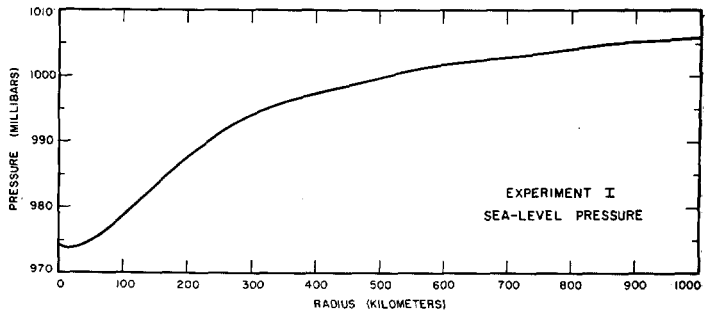

FIGURE 2.—Experiment I, sea level pressure as a function of radius.

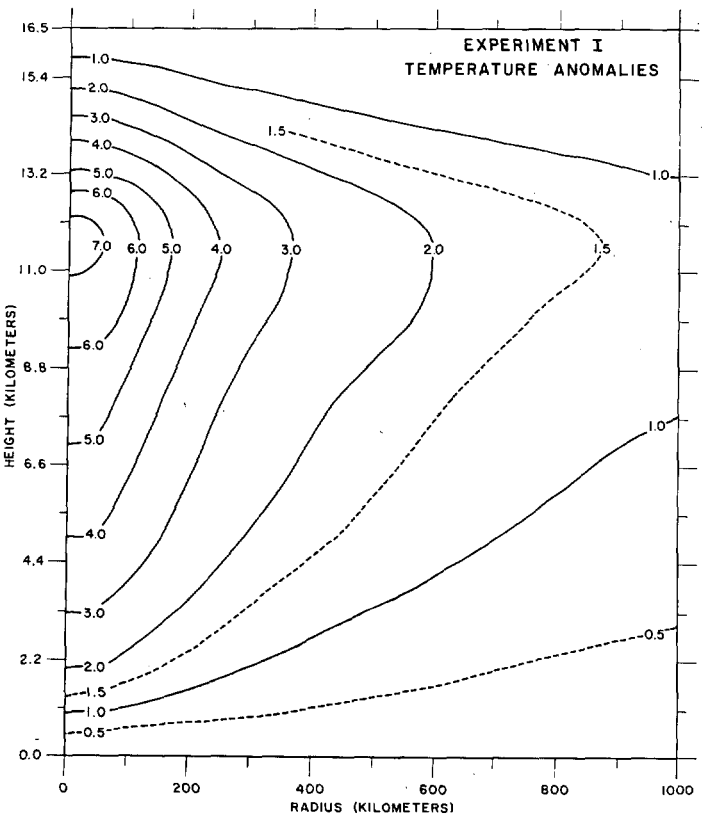

FIGURE 1.—Experiment I, vertical cross-section of the temperature anomaly (°K.) from the mean tropical atmosphere.

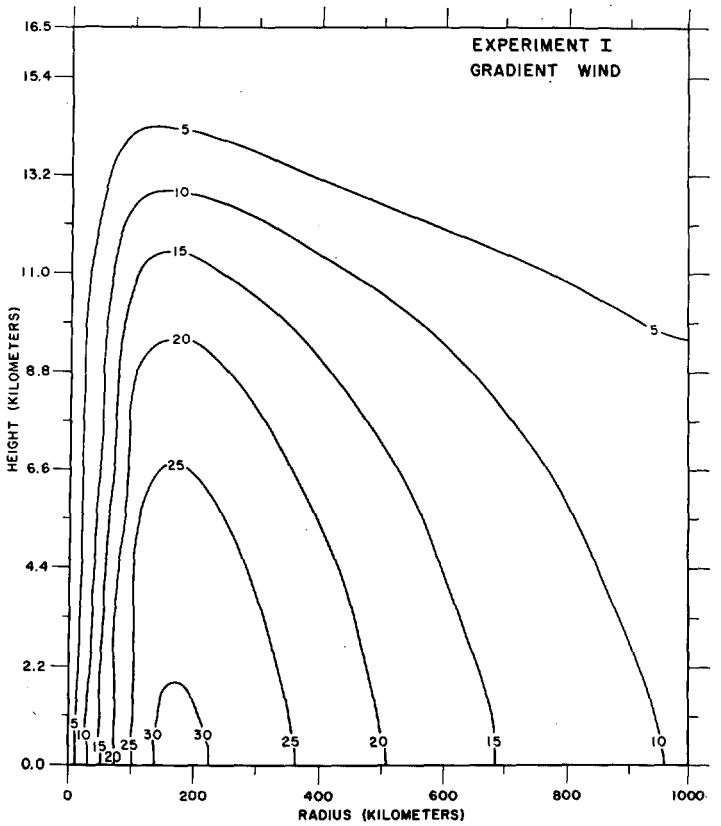

FIGURE 3.—Experiment I, vertical cross-section of the gradient wind v_θ in units of meters per second.

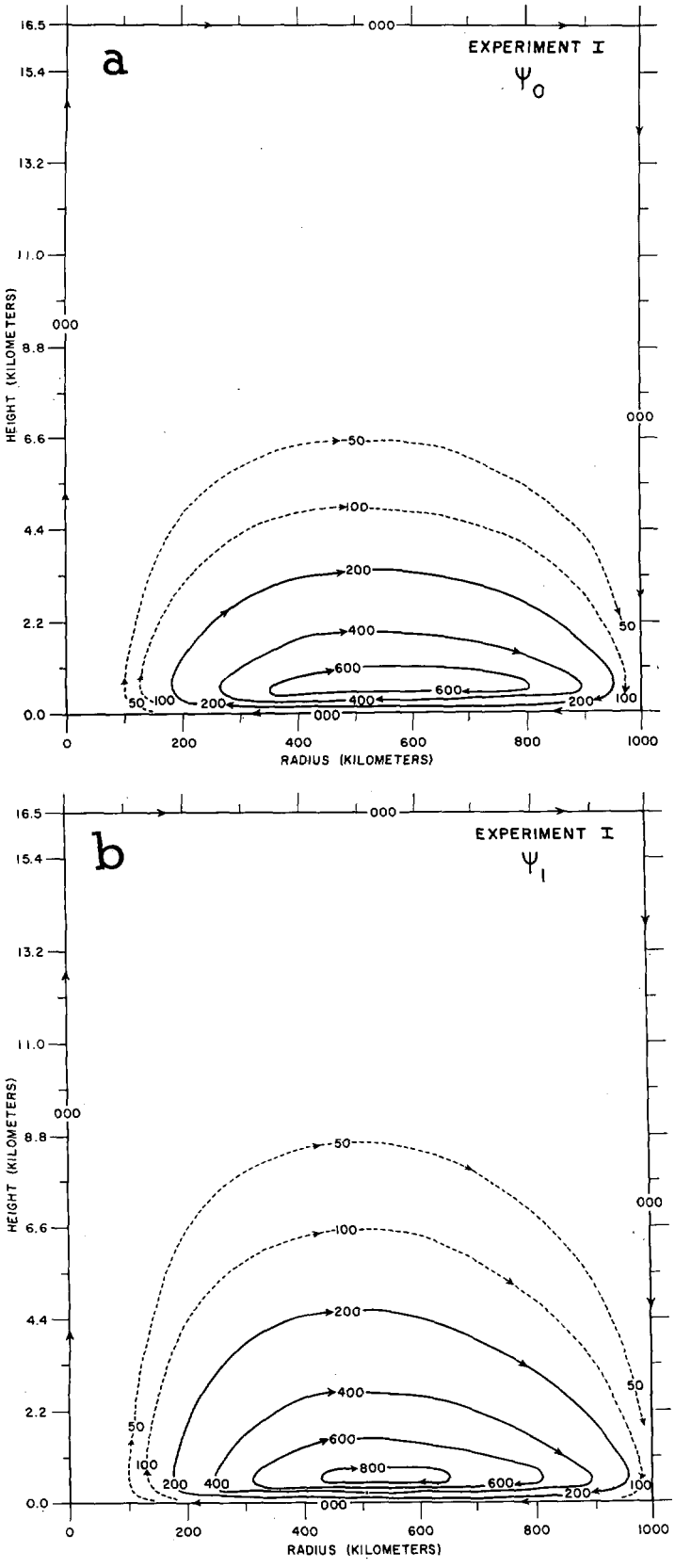

FIGURE 4.—Experiment I, vertical cross-sections of (a) ψ_0, (b) ψ_1, and (c) ψ_2. Units are tens of kilotons per second.

are applied to ψ_0. Figure 5 shows the vertical velocities associated with each of these stream functions. Notice that close to the vortex center w_1, is smaller than both w_0 and w_2. This oscillation in the corrections to w would lead one to suspect that a solution based solely on the first few wet corrections might be in error.

Figure 6 shows (a) the ratio $k_1=\Delta_2\psi/\Delta_1\psi$, (b) the dry static stability $\partial\theta/\partial z$, and (c) the wet static stability $(\partial\theta/\partial z)+(L/\phi)(\partial q_{ss}/\partial z)$. We note that k_1 shows a variation with static stability which is inverse to that predicted by Eliassen [3]. Largest values of k_1 occur in the high troposphere where the static stability is largest. k_1 decreases downward from this region as the static stability also decreases. The fact that k_1 is negative close to the vortex center and greater than one in the high troposphere is an extremely disturbing result. It is clear that Eliassen's deductions concerning the behavior of the k-values are not valid for this particular vortex.

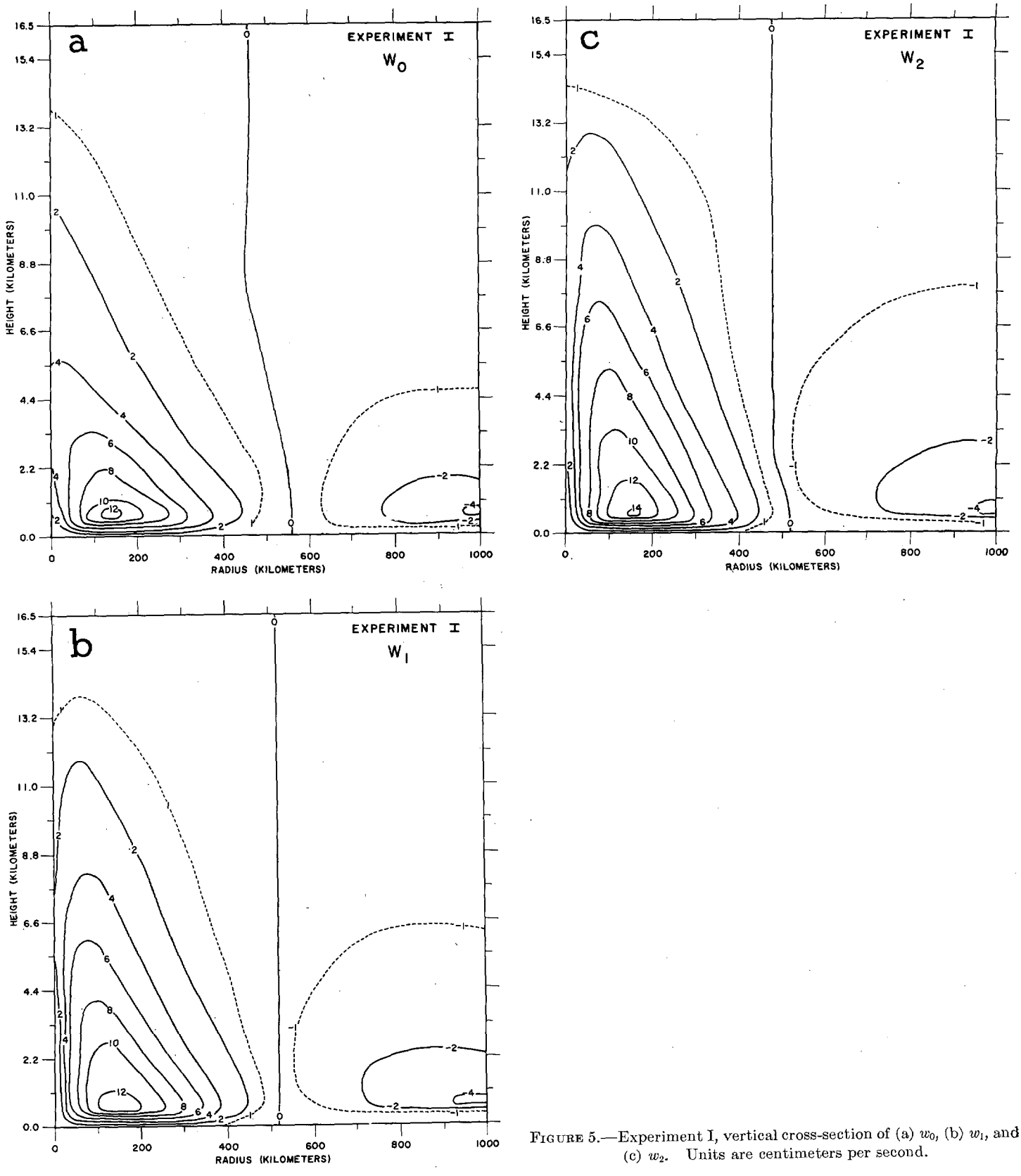

FIGURE 5.—Experiment I, vertical cross-section of (a) w_0, (b) w_1, and (c) w_2. Units are centimeters per second.

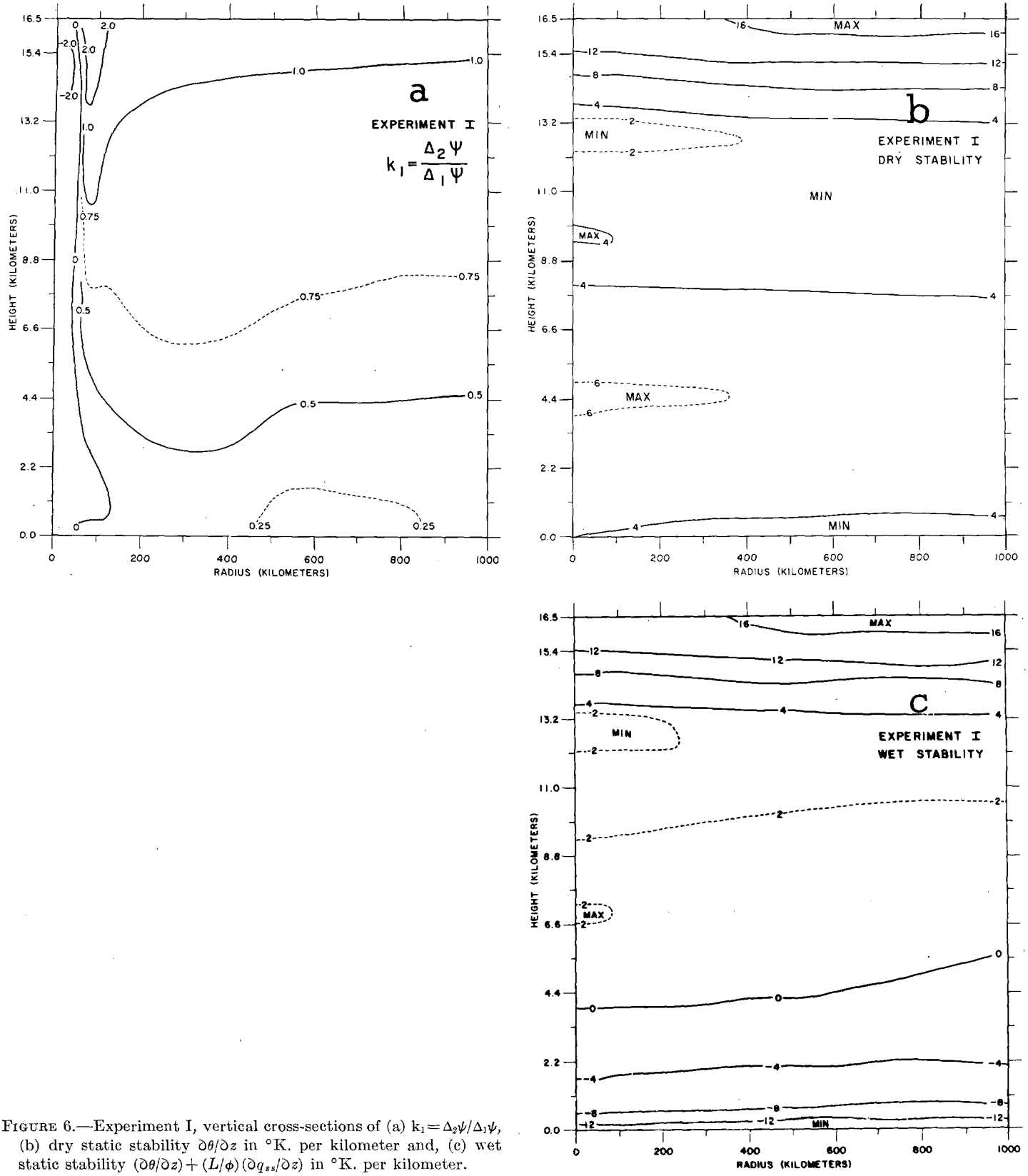

FIGURE 6.—Experiment I, vertical cross-sections of (a) $k_1 = \Delta_2\psi/\Delta_1\psi$, (b) dry static stability $\partial\theta/\partial z$ in °K. per kilometer and, (c) wet static stability $(\partial\theta/\partial z) + (L/\phi)(\partial q_{ss}/\partial z)$ in °K. per kilometer.

7. EXPERIMENT II

In Experiment II (which was carried out for a weaker vortex), ψ_0, $\Delta_1\psi$, $\Delta_2\psi_1$ . . ., $\Delta_{26}\psi$ were calculated. In view of the fact that $\Delta_{26}\psi$ was smaller than the tolerance employed to terminate each individual relaxation, $\psi_{26}=\psi_0+\Delta_1\psi+\Delta_2\psi+\ \ldots\ +\Delta_{26}\psi$ was considered to be ψ, the solution of the boundary value problem. We feel that the fact that we were able to obtain convergence to within the relaxation tolerance is evidence in support of Eliassen's contention that equation (24) will, at least in some cases, give the solution to the wet boundary value problem.

The temperature anomalies, the sea level pressure profile, and the gradient winds for Experiment II are shown, respectively, by figures 7, 8, and 9. K_z, at sea level, was set equal to 10 m.^{2} sec.$^{-1}$ and allowed to vary in a linear fashion to zero at the 100-mb. surface. C_D and T_{sea} have the same values as in Experiment I. Figure 10 shows ψ_0, ψ_1, ψ_{14}, and ψ_{26}. The general vertical expansion of the circulation with successive corrections, noted in Experiment I, is also found here. ψ_{14} is shown because $v_{r_{14}}$ differs from $v_{r_{26}}$ by less than decimeters per second and w_{14} differs from w_{26} by less than centimeters per second. ψ_{14} would probably be adequate input to our prognostic model.

Figure 11 shows w_0, w_1, w_{14}, and w_{26}. We will not discuss this figure in detail but, instead, go directly to a discussion of figure 12 which illustrates k_1, k_2, k_3, and k_4 where

$$k_\nu=\frac{\Delta_{\nu+1}\psi}{\Delta_\nu\psi} \tag{35}$$

and figure 13 which shows the wet and dry static stabilities for Experiment II. These two figures, together with figure 6, strongly support the conclusion that the k_ν tend to increase in magnitude with increasing static stability.

Figure 12 shows that the magnitude of k_1 exceeds unity over a substantial portion of the troposphere. Note, however, that the area covered by $|k_\nu|>1$ diminishes

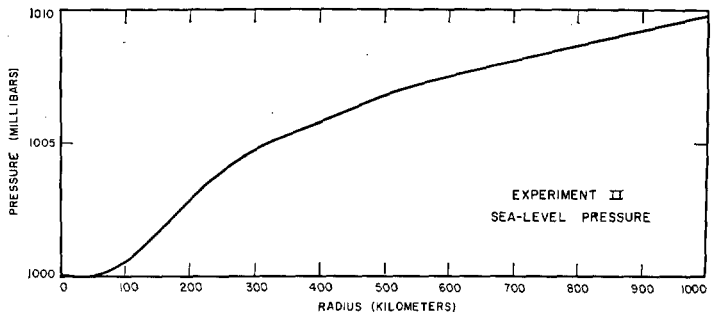

FIGURE 8.—Experiment II, sea level pressure as a function of radius.

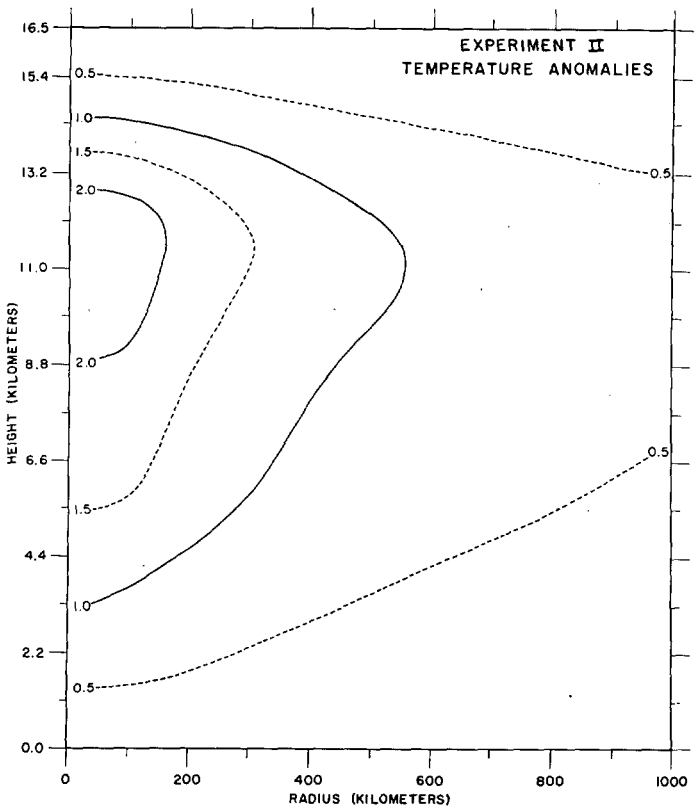

FIGURE 7.—Experiment II, vertical cross-section of temperature anomaly (°K.) from the mean tropical atmosphere.

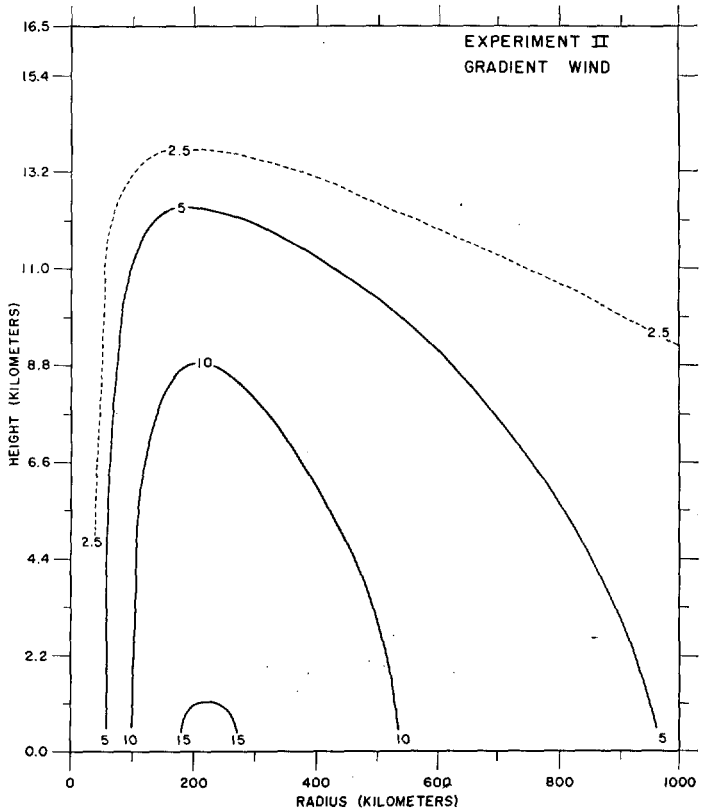

FIGURE 9.—Experiment II, vertical cross-section of the gradient wind v_θ in units of meters per second.

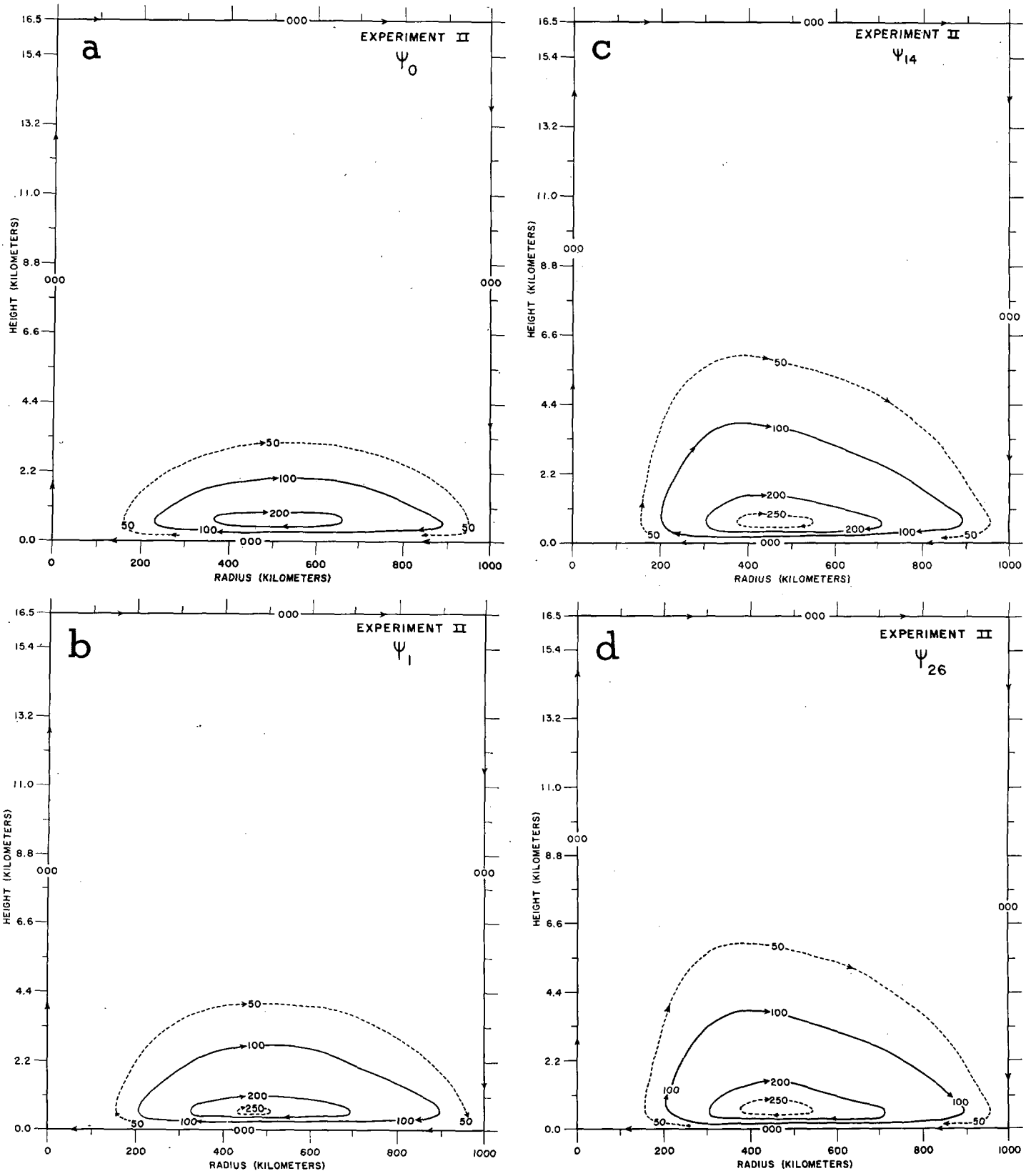

FIGURE 10.—Experiment II, vertical cross-sections of (a) ψ_0, (b) ψ_1, (c) ψ_{14}, and (d) ψ_{26}. Units are tens of kilotons per second.

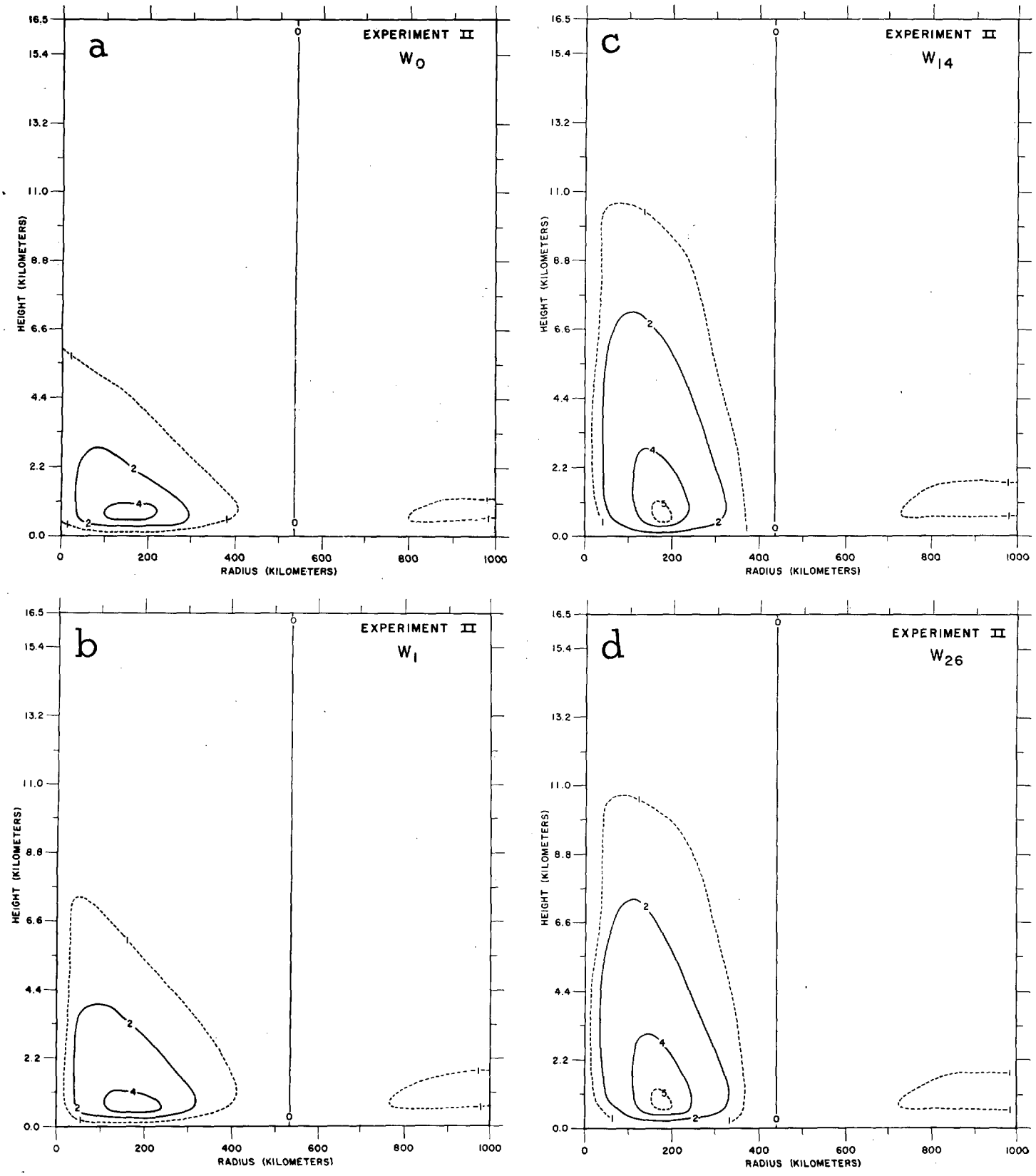

FIGURE 11.—Experiment II, vertical cross-sections of (a) w_0, (b) w_1, (c) w_{14}, and (d) w_{26}. Units are centimeters per second.

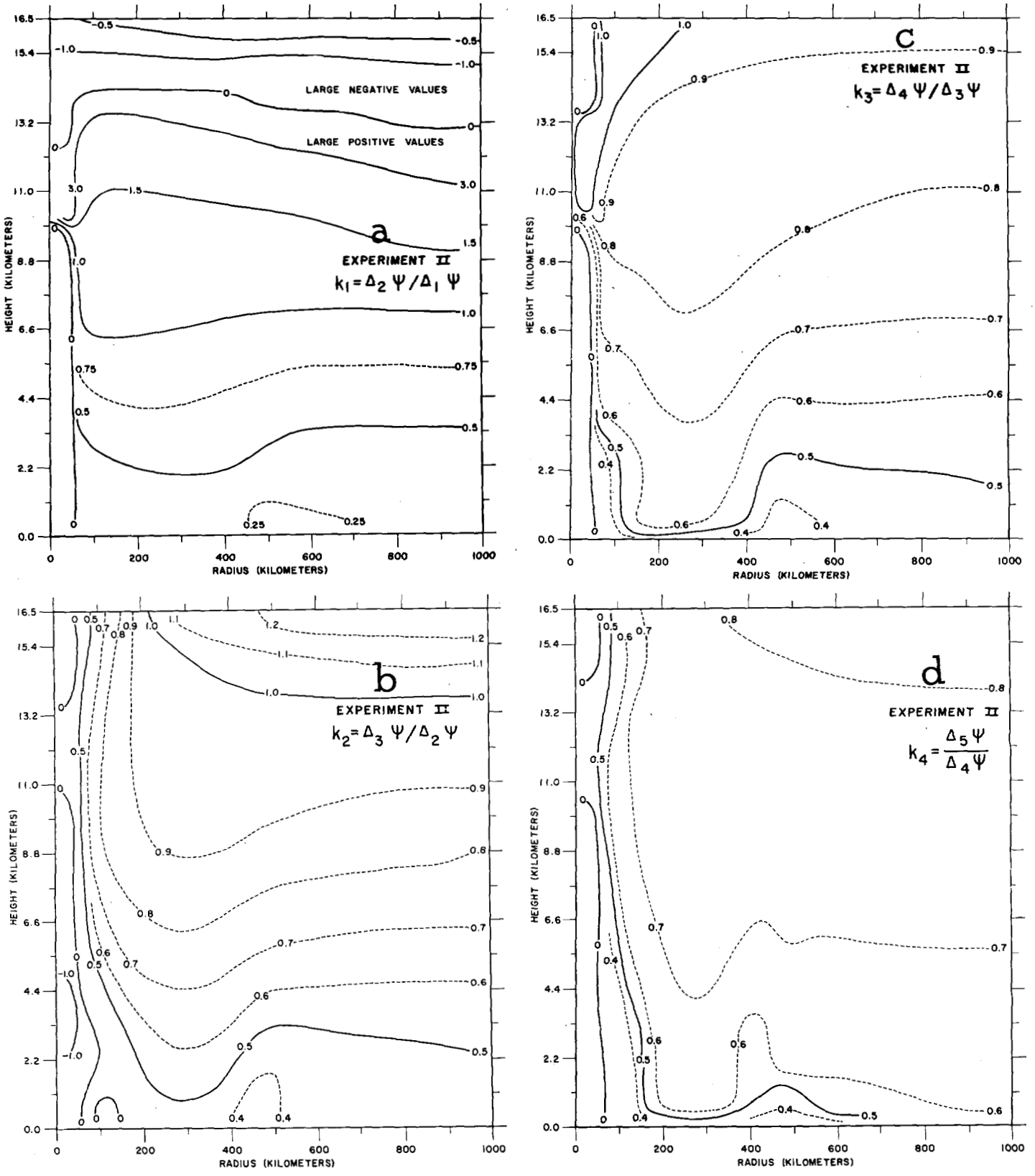

FIGURE 12.—Experiment II, vertical cross-sections of (a) $k_1=\Delta_2\psi/\Delta_1\psi$, (b) $k_2=\Delta_3\psi/\Delta_2\psi$, (c) $k_3=\Delta_4\psi/\Delta_3\psi$, and (d) $k_4=\Delta_5\psi/\Delta_4\psi$.

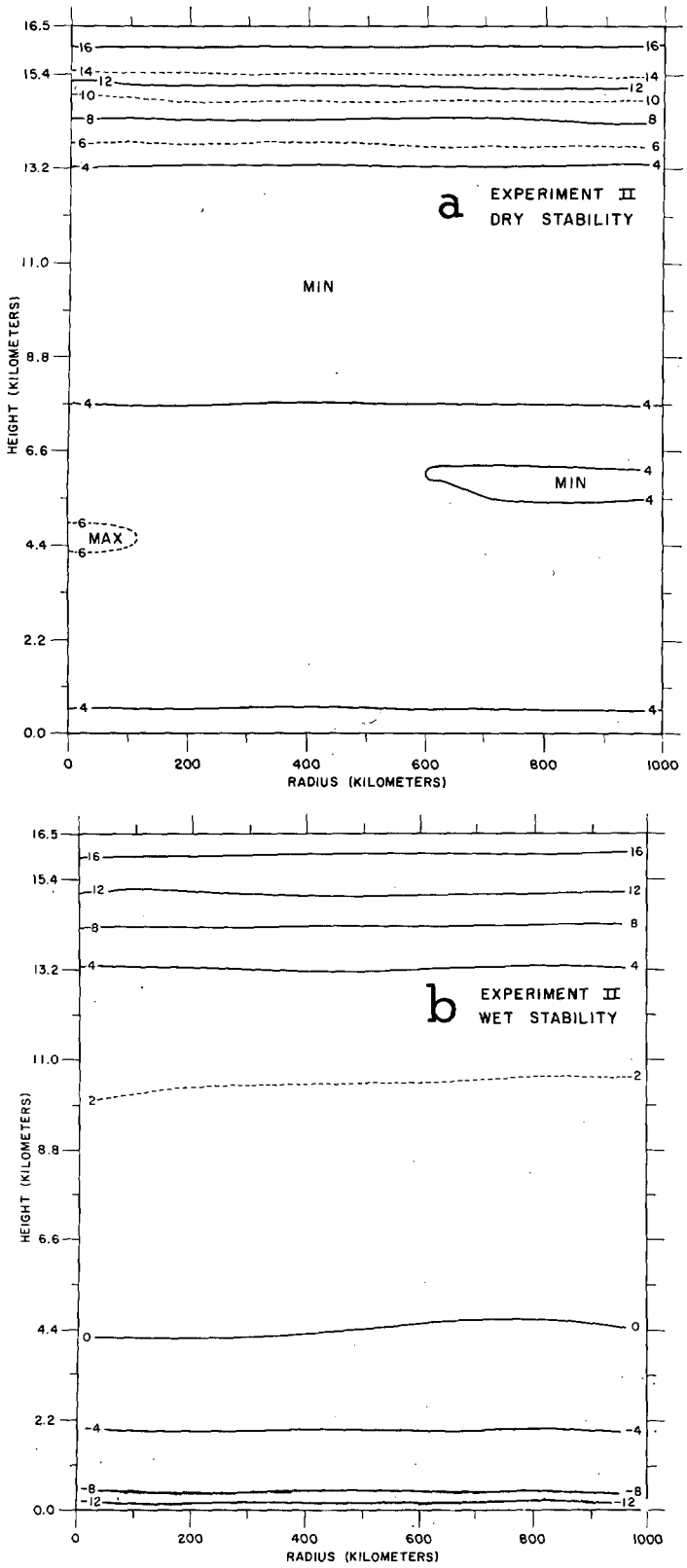

FIGURE 13.—Experiment II, vertical cross-sections of (a) dry static stability $\partial\theta/\partial z$, and (b) wet static stability $(\partial\theta/\partial z)+(L/\phi)(\partial q_{ss}/\partial z)$. Units are °K. per kilometer.

as ν increases. Oscillations in the sign of $\Delta_\nu\psi$ are illustrated by the negative values of k_ν found close to the vortex center in all four cross-sections and in the negative values of k_1 found in the high troposphere. In the case of k_1, changes in sign, especially those in the high troposphere, seem to be accompanied by a zero order discontinuity in k_1. Although not shown here, no negative values of k_ν were observed for $\nu>8$. Ratios in excess of unity were also absent for the larger values of ν.

Interestingly enough, the spatial variation of k_ν tended to vanish as ν became larger. The spatial distributions of k_{12} through k_{25} were remarkably uniform. However, the k_ν continued to vary with ν. Hence, even for the high-order corrections, equation (25) could not be applied with success.

8. CONCLUSIONS

For the vortex studied in Experiment II, it was possible to obtain balanced meridional velocity components from the iterative scheme suggested by Eliassen. However, the series produced by the iterations was not geometric nor did the ratio of a given correction to its predecessor decrease with increasing static stability as predicted by Eliassen. This was also the case in Experiment I. At some grid points, ratios of successive low-order corrections exceeded unity in magnitude.

ACKNOWLEDGMENTS

The author wishes to express his gratitude to his colleagues, Messrs. James W. Trout and Walter J. Koss for helpful discussions on various phases of the research reported on above.

REFERENCES

1. A. Eliassen, "Slow Thermally or Frictionally Controlled Meridional Circulations in a Circular Vortex," *Astrophysica Norvegica*, vol. 5, No. 2, May 1952, pp. 19–60.
2. A. Eliassen, "Remarks on the Problem on Long Range Weather Prediction," *Dynamics of Climate*, (Proceedings of a Conference on the Application of Numerical Integration Techniques to the Problem of the General Circulation, Oct. 1955), Pergamon Press, New York, 1960, pp. 37–43.
3. A. Eliassen, "On the Formation of Fronts in the Atmosphere," *The Atmosphere and the Sea in Motion*, Rockefeller Institute Press with Oxford University Press, New York, 1959, pp. 277–287.
4. M. A. Estoque, "Vertical and Radial Motions in a Tropical Cyclone," *Tellus*, vol. 14, No. 4, Nov. 1962, pp. 394–402.
5. C. L. Jordan, "Mean Soundings for the West Indies Area," *Journal of Meteorology*, vol. 15, No. 1, Feb. 1958, pp. 91–97.